Available online at www.sciencedirect.com
SCIENCE DIRECT
Tetrahedron
ELSEVIER
Tetrahedron 61 (2005) 2431–2440

Conformational behavior of dithia[n.3.3](1,3,5)cyclophanes and dithia[n.3.3](1,2,6)cyclophanes

Jian-Wei Xu,[a] Ting-Ting Lin[a] and Yee-Hing Lai[b,*]

[a]*Institute of Materials Research and Engineering, 3 Research Link, Singapore 117602*
[b]*Department of Chemistry, National University of Singapore, 3 Science Drive 3, Singapore 117543*

Received 7 September 2004; revised 6 December 2004; accepted 7 January 2005

Available online 28 January 2005

Abstract—The conformational behavior of a series of crown-fused dithia[n.3.3](1,2,6)cyclophanes (**126-CPs**) and dithia[n.3.3](1,3,5)-cyclophanes (**135-CPs**) was investigated by variable-temperature ^{1}H and ^{13}C NMR spectroscopy, X-ray crystallography and density functional theory (DFT) calculations. Single crystal X-ray structure analysis showed that two thia-bridges in **126-CPs** adopted a *pseudochair–pseudochair* (*cc*) conformation and the cyclophane decks underwent a ring-tilting motion in the case of [10.3.3](1,2,6)cyclophane (**1a**). In contrast, the thia-bridges in **135-CPs** took both *cc* and *pseudoboat–pseudochair* (*bc*) conformations, and the ring-tilting process was also found in [10.3.3](1,3,5)cyclophane (**2a**). Variable temperature ^{1}H NMR study revealed that there was no wobbling-motion for two thia-bridges in **126-CPs** while thia-bridges in **135-CPs** experienced a wobbling-process with a conformational barrier of 9.21 and 8.80 kcal mol^{-1}, respectively, for **2a** and [13.3.3](1,3,5)cyclophane (**2b**). DFT calculations for the two cyclophanes series revealed that **126-CPs** preferred a *cc* conformation which was consistent with the experimental observation; similarly, **135-CPs** took a preferential *cc* conformation, agreeing with **2a** having a predominant *cc* conformer (*cc*:*bc* ratio = 70:30), but not **2b** having a predominant *bc* conformer (*cc*:*bc* ratio = 15:85) in the solid state.

1. Introduction

Conformational analysis plays an important role in cyclophane chemistry.[1] The understanding of preferred conformations in cyclophane (**CP**) is of importance in the design of various supramolecular systems. Small-sized **CP** molecules, such as, 2,11-dithia[3.3]metacyclophane (**MCP**)[2–6] frequently act as a model to explore the mobility of such **CPs** due to the presence of a variety of conformational processes including ring-flipping, ring-tilting, bridge-wobbling and *syn-anti* isomerization. It is well understood that the conformational characteristics of [3.3]**MCP** are dependent particularly upon the 'internal' (9, 18-position) substitution, the attribute of the 'internal' atom and the nature of the bridge heteroatoms (Chart 1).[7–10] The 'internal' substituents in [3.3]**MCP** are able to direct its conformation preference when non-covalent interaction such as hydrogen bonding between substituents and bridges is present.[8] For example, 9-amino-2,11-dithia[3.3]**MCP**, being different from its precursor *syn*-9-nitro-2,11-dithia[3.3]**MCP**, is *anti*. However, 9-18-diamino-2,11-dithia[3.3]**MCP** shows *syn* and its thia-bridges adopt a *pseudoboat–pseudoboat* (*bb*) conformation as a result of the formation of an intramolecular hydrogen-bonding network. Likewise, 9-amino-18-nitro-2,11-dithia[3.3]**MCP** takes a *pseudoboat–pseudochair* (*bc*) conformation due to the presence of an intramolecular S···H–N hydrogen bonding. Other factors such as the dipole moment of a molecule sometimes may have an effect on the predominant conformation.[11]

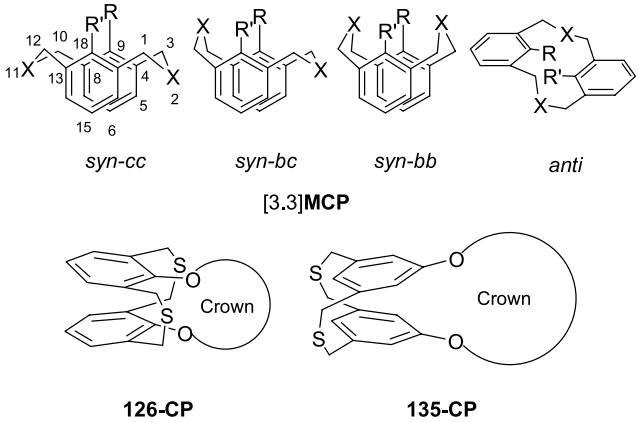

Chart 1.

Keywords: Conformation; (1,3,5)Cyclophane; (1,2,6)Cyclophane.
* Corresponding author. Tel.: +65 6874 2914; fax: +65 6779 1691; e-mail: chmlaiyh@nus.edu.sg

0040–4020/$ - see front matter © 2005 Elsevier Ltd. All rights reserved.
doi:10.1016/j.tet.2005.01.027

On the other hand, examples of the synthesis and conformational analysis of multibridged cyclophanes were studied 30 years ago. Boekelheide first reported the synthesis of 2,11,20-trithia[3_3](1,3,5)**CP**[12] in which one thia-bridge underwent a wobbling-process in the solid state.[13] Shinmyozu studied the synthesis and conformational behavior of [3_3](1,3,5)**CP**, in which one bridge experienced a wobbling-process with an activation energy barrier of 12.4 kcal mol^{-1}.[14] Fluorine-substituted [3_3](1,3,5)**CP** whose π–π absorption bands correlate to the number of fluorine atoms were also investigated.[15] Bodwell reported the synthesis of [n.3.3](1,3,5)**CPs** as tethered [2.2]**MCPs** precursors with various lengths of alkyl tether.[16,17] Recently, our interest has focused on the synthesis and complexation properties of crown-fused dithia[n.3.3](1,2,6)**CPs** (**126-CPs**) and dithia[n.3.3]-(1,3,5)**CPs** (**135-CPs**) (Chart 1).[18–20] Their binding properties towards alkali metal ions largely relate to the ring-tilting motion of two aromatic rings. Herein we wish to further report the syntheses, X-ray crystal structure and the conformational analysis of crown-fused **126-CPs** and **135-CPs** in solution by variable-temperature ^{1}H and ^{13}C NMR spectroscopy. The energy-minimized structures based on the DFT calculations are presented and compared with those from the X-ray crystallography and variable-temperature NMR spectroscopy.

2. Results and discussion

2.1. Synthesis of 126-CPs and 135-CPs

First, **1a** and **1b** were synthesized as shown in Scheme 1. Compound 2,6-diformylphenol **3**, which was prepared by tetrabromination of 2,6-dimethylphenol acetate followed by hydrolysis in NaOAc/HOAc,[21] was used as a starting material. Compound **5a** was obtained in a 48% yield when the reaction temperature was maintained at 60–70 °C and the mixture stirred for 24 h. A near quantitative yield of tetrol **5b** was obtained by reducing **5a** with $NaBH_4$ in refluxing THF. Treatment of **5b** with phosphorus tribromide in dry CH_2Cl_2 readily gave tetrabromide **5c** in 80% yield. Finally **1a** was obtained by intramolecular cyclization of **5c** with Na_2S under high dilution conditions. The method of preparation of **1b** was the same as that of other analogs **1c–d**.[18,19]

The synthesis of **2a–c** was attempted (Scheme 2). First, compound **9** was prepared from bromomethylation of 2,4,6-trimethylanisole in 47% HBr/HOAc in the presence of a phase transfer catalyst *N*,*N*,*N*-trimethyltetradecyl ammonium bromide.[22] Compound **9** was converted to **10** by reacting with thiourea followed by hydrolysis in refluxing 10% KOH aqueous solution. The compound

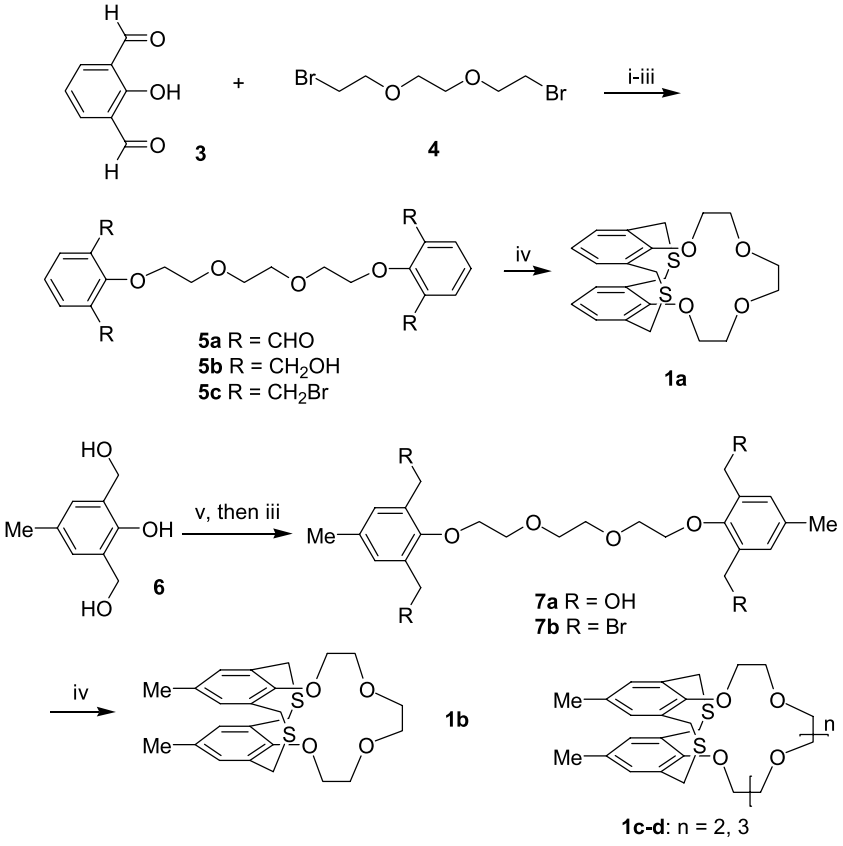

Scheme 1. The synthetic route for **1a–b**. Reagents and conditions: (i) K_2CO_3, DMF, 60–70 °C; (ii) $NaBH_4$, THF, reflux; (iii) PBr_3, CH_2Cl_2, 0 °C; (iv) Na_2S, ethanol/benzene, high dilution conditions, rt; (v) $Br(CH_2CH_2O)_2CH_2CH_2Br$, K_2CO_3, acetone, reflux.

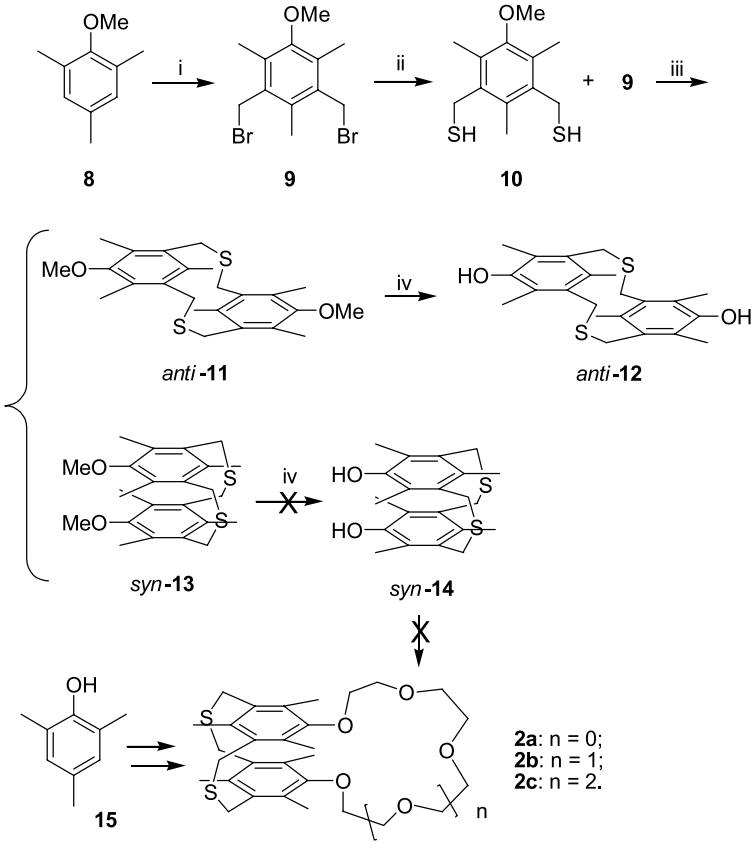

Scheme 2. The synthetic route for **2a**–**c**. Reagents and conditions: (i) 1,3,5-trioxane, HOAc, aq HBr (48%), 95 °C; (ii) $(NH_2)_2CS$, aq KOH, reflux, 9 M H_2SO_4; (iii) KOH, benzene, ethanol, high dilution conditions, rt; (iv) BBr_3, CH_2Cl_2.

syn-**13**, together with its isomer *anti*-**11** was prepared from the cross-coupling reaction of dibromide **9** and dithiol **10** under high dilution conditions. The two isomers could be readily separated by column chromatography. Demethylation of *anti*-**11** was carried out using BBr_3 in CH_2Cl_2 to afford *anti*-**12**. A similar reaction attempted using the isomer *syn*-**13** however was unsuccessful. The significant steric hindrance of the *ortho*-methyl and opposite aryl groups might have discouraged the reaction. An alternative synthesis of **2a**–**c** was achieved starting from 2,4,6-trimethylphenol **15** which reacted with polyethylene glycol dibromide, followed by tetrabromomethylation and intramolecular cyclization with sodium sulfide to afforded **2a**–**c**.[20]

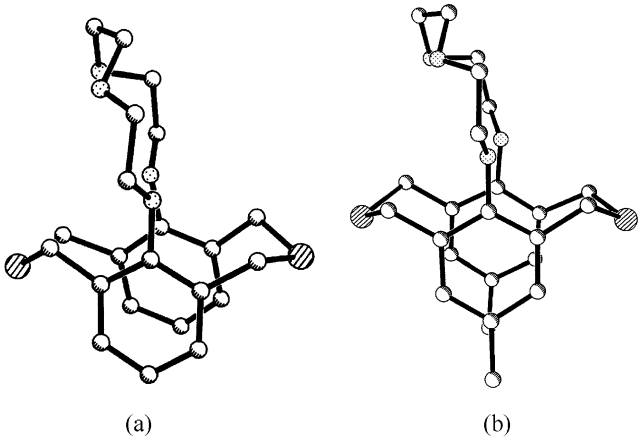

Figure 1. ORTEP drawings of (a) **1a**-(**I**) and (b) **1b**.

2.2. Crystal structures of 126-CPs and 135-CPs

The X-ray single crystal structures of **1a**–**d** and **2a**–**b** were determined. All the single crystal structures of **1a**–**d** clearly showed a *pseudochair–pseudochair* (*cc*) conformation for both thia-bridges. Their normal C–S bond lengths and C–S–C bond angles were similar and close to expected values.[23–26] It was noteworthy that **1a** showed that there were two different non-interconverting structures **1a**-(**I**) and **1a**-(**II**) in the crystalline state. The ORTEP drawings of **1a**-(**I**) and **1b** are illustrated in Figure 1. However, **1a**(**I**) and **1a**(**II**) did not exhibit significant differences between their bond lengths, bond angles and thia-bridge conformations. Figure 2 clearly manifests the ring-tilting process in **1a**. Analysis of other single crystal structures of **1c**–**d** showed the same *cc* conformation for thia-bridges and no disorder of thia-bridges was observed.[18,19] This appears to indicate that the wobbling process of thia-bridges is restricted by the 'internal' substitution for **126-CPs** series.

Similar to **1a**, two independent conformers (**2a**-(**I**) and **2a**-(**II**)) of **2a** were also found in the crystalline state and one of the two thia-bridges in a conformer (**2a**-(**II**)) was triply disordered.[20] Both thia-bridges in **2a**-(**II**) adopted the *pseudochair* conformation with C–S bond lengths and C–S–C bond angles very close to those observed in **1a**. Nevertheless, in conformer **2a**-(**I**), one thia bridge was

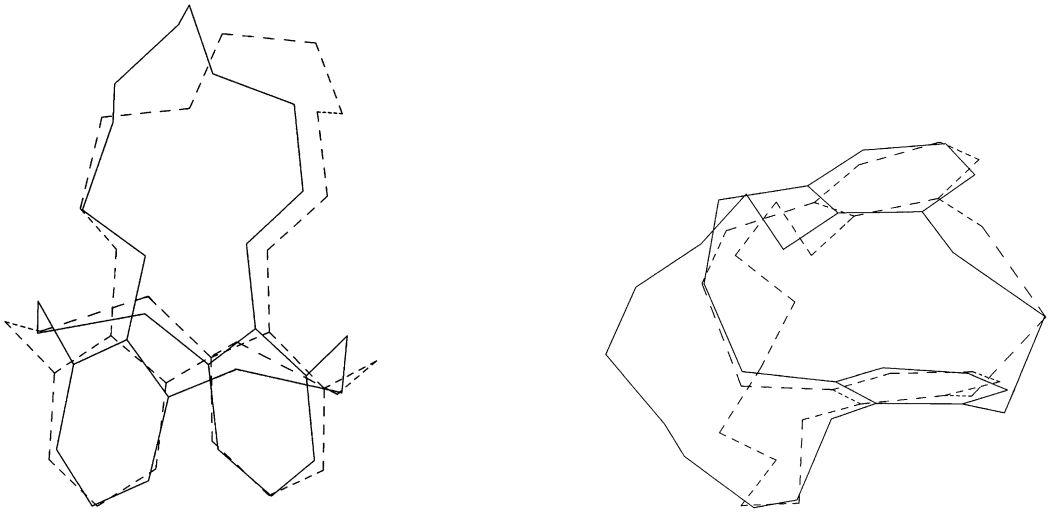

Figure 2. A diagram illustrating the tilting motion in the two conformers of **1a**-(**I**) and **1a**-(**II**). Two independent structures are indicated by solid line and dashed line, respectively.

Table 1. A comparison of the dihedral angles of two aryl rings and the centroid–centroid distances of aromatic rings in **1a–d**, **2a–b** and compound **16**

CP	Dihedral angle of two aryl rings (°)	Centroid–centroid distance of two aryl rings (Å)
1a-(**I**)	16.2	3.50
1a-(**II**)	15.5	3.49
1b	14.2	3.49
1c	13.4	3.45
1d	12.8	3.43
2a-(**I**)	16.1	3.59
2a-(**II**)	13.6	3.55
2b	12.9	3.56
16	<1	3.19

'normal' but the sulfur atom in the second was triply disordered with an occupancy ratio of 0.4:0.3:0.3. The observation indicates a possible inter-conversion among *bc* and *cc* conformations in the solid state. Similarly, one of thia-bridges in **2b** was disordered, resulting in a **2b**-*bc* conformation as a major component (85%). The coexistence of *bc* and *cc* conformers has also been found previously[12,13] except that the *cc* conformation was the predominant isomer (80%). In comparison to the conformers in **2a** with a ratio of 70:30 (*cc*:*bc*, inclusive of **2a**(**I**) and **2a**(**II**)), **2b** with a ratio of 15:85 (*cc*:*bc*) has significantly more preference for the *bc* conformer. In addition to the probable effect of crystal packing, we believe this is in part as a result of the great difference in their ground state energies, that is, an increase in ground state energy going from *bc* to *cc*.

There is a possible explanation why a wobbling-process in one of the thia-bridges was only observed for **2a** and **2b** but not in the series of **126-CPs**. In **1a**, for example, the *bc* conformation would experience a significant steric repulsion between the *pseudo-boat* sulfur atom and the central phenolic oxygen atom in the crown ether moiety and thus the strong preference for only the *cc* conformer. In contrast, in **2a–b** a pair of similar steric interactions would be experienced in both the *cc* and *bc* conformations, thus the

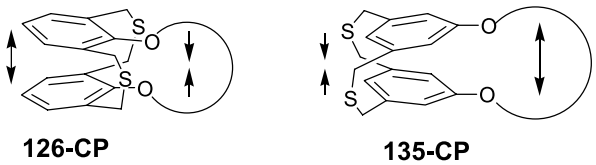

Figure 3. The tilting process of **126-CPs** and **135-CPs**.

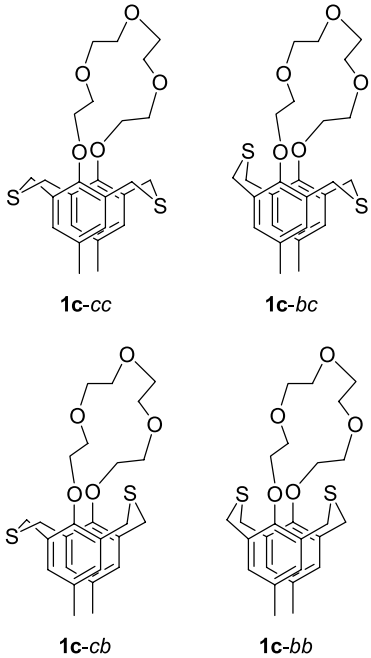

Figure 4. The possible conformation of **1c** in solution.

disorder in one of the thia-bridges even in the solid state was observed. On the basis of a buttressing effect, the *cc* conformation would be relatively less stable, and thus **135-CPs** have a preference to the propelling *bc* conformation similar to that observed[13] of which one of the sulfur bridges experiences rapid wobbling.

The benzene rings in all **126-CPs** and **135-CPs** in the solid state were not parallel to each other. The centroid arene–arene stacking (interplanar) distances and dihedral angles (tilting angle) for aromatic rings are summarized in Table 1. The interplanar distances were slightly larger than the normal arene–arene stacking distance of 3.4 Å. Unlike 2,11,20-trithia[3_3](1,3,5)**CP**[12] (**16**) in which two benzene rings are nearly parallel, the two benzene rings in each of **2a** and **2b** were tilted at an angle in the range of 12.9–16.1° in the reverse manner to **126-CPs** (Fig. 3). There was also a decreasing trend in dihedral angle going from **2a** to **2b**. The decrease in tilting dihedral angle following an increase in chain length of the crown ether link could be explained by an increasing demand for a larger cavity size of the crown ether. A smaller dihedral angle going from **1a** to **1b** is however not understood. If the steric demand of the methyl groups in **1b** is taken into consideration, the dihedral angle in **1b** would be expected to be larger. In this series of **126-CPs**, an identical transannular distance accompanied by a varying dihedral angle of two aryl rings indirectly supports a breathing mechanism (in solution)[19] of the crown ether unit

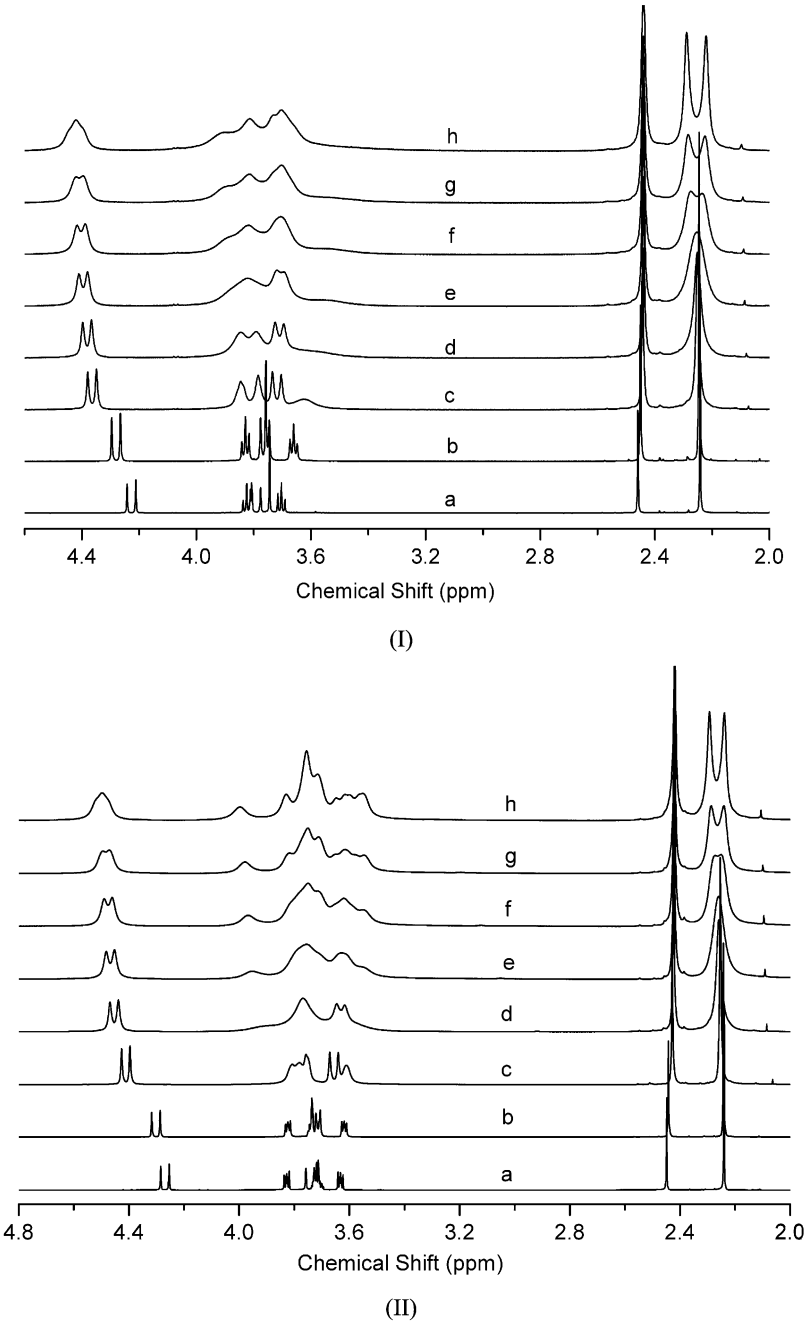

Figure 5. The variable temperature ^{1}H NMR spectra of (I) **2a**: (a) 300, (b) 253, (c) 203, (d) 193, (e) 188, (f) 185, (g) 183 and (h) 178 K; and (II) **2b**: (a) 300 K, (b) 273 K, (c) 213 K, (d) 193 K, (e) 188 K, (f) 185 K, (g) 183 K and (h) 178 K in CD_2Cl_2.

as described. The change in dihedral angle would result in a change in the conformation and cavity size of the crown ether and thus its complexation ability.

2.3. Dynamic NMR spectroscopy study

Although **1a**–**d** take the *cc* conformations as observed in the solid state, it is not possible to rule out the wobbling processes *cc* ⇔ *bc* ⇔ *cb* ⇔ *bb* as well as their diastereotopic conformers of thia-bridges in solution as illustrated in Figure 4 using **1c** as an example. Therefore we examined the dynamic NMR (500 MHz) spectra of **1a**–**d** over the temperature range from 298 to 178 K, however we did not observe the freezing of this wobbling process of the thia-bridges indicating either a relatively low energy conversion barrier or less opportunity to adopt *bc*, *cb*, or *bb* due to the electronic repulsion between sulfur and phenolic oxygen. Thus, it would be more interesting to find out whether the bridge wobbling processes of the thia-bridges in **135-CPs** series could be observed. The aryl rings in **135-CPs** are hexa-substituted and thus the relatively higher steric demand might allow observation of the freezing of the bridge wobbling processes at a reasonable temperature within the experimental limitations.

The temperature-dependent ^{1}H NMR (500 MHz) spectra of **2a** were recorded in CD_2Cl_2 in the temperature range of 178–300 K (Fig. 5(I)). In general the NMR signals broadened significantly as the temperature was lowered from 300 to 178 K. Although the oxyethylene protons in the crown unit were clearly resolved at 300 K, broadening of these signals upon cooling led to weak and overlapped signals. This phenomenon is however consistent with a slowing down of the conformational processes in the macroring. The diastereotopic bridge methylene protons (–CH_2SCH_2–) also appeared clearly as an AB quartet at δ 4.23 and 3.79 at room temperature. These signals broadened and finally coalesced at about 180 K. They were expected to reappear as two separate AB quartets at the low temperature limit, but in our study, the limitation of the temperature was near 175 K at which these signals were not fully resolved. Actually, a broad incipient triplet was observed in both spectra of **2a** and **2b** at 178 K.

The methyl protons in **2a** appeared as two singlets at δ 2.46 and 2.24 in an integration ratio of 1:2 at room temperature. Thus, the latter could be readily assigned to the two methyl groups adjacent to the crown ether unit. The two methyl groups were certainly also adjacent to the two thia-bridges and thus could be used as proton probes for the conformational analysis of the bridge wobbling processes by dynamic ^{1}H NMR spectroscopy. As the temperature was lowered, the signals corresponding to this pair of methyl groups (at δ 2.24 at 300 K) broadened and coalesced at 186 K. This signal became gradually resolved again as the temperature was further lowered and reappeared as two singlets at δ 2.26 and 2.22 at 178 K. This in fact indicates the freezing out of the wobbling processes of the thia-bridges, leading to a conformation in which the two initially (room temperature) identical methyl groups are now magnetically non-equivalent. The dynamic NMR study of **2b** revealed a similar phenomenon (Fig. 5(II)). An analysis of the general conformational behavior will be discussed using **2b** as an example.

In the analysis of a conformational process using dynamic NMR spectroscopy the free energy of activation ($\Delta G_c^{\neq}$), which represents the conformational barrier, could be estimated by the coalescence temperature method. Employing a pair of non-coupled signals as the probe for conformational analysis, the value of $\Delta G_c^{\neq}$ could be derived from the Eyring equation:[27]

$$k_c = 0.707\pi\Delta\nu$$

$$\Delta G_c^{\neq} = 2.303RT_c(10.319 + \log T_c - \log k_c)$$

Where $\Delta\nu$ is the frequency difference at the low temperature limit, T_c is the coalescence temperature and $\Delta G_c^{\neq}$ is the transition state free energy at coalescence temperature.

Although the crown ether link in **2b** is relatively longer than that in **2a** their conformational barriers for the thia-bridge wobbling processes seem to be very similar (Table 2). These barriers are in fact relatively lower than that observed for a similar wobbling process in [3.3]-**MCP** (10.8 kcal mol^{-1}).[5] In contrast, similar bridge wobbling processes of aza-bridges in *N*,*N*,*N*-tritosyl-2,11,20-triaza[3$_3$](1,3,5)**CP** (13.6 kcal mol^{-1})[28] and [3$_3$](1,3,5)**CP** (12.4 kcal mol^{-1})[14] however, involved a higher energy barrier.

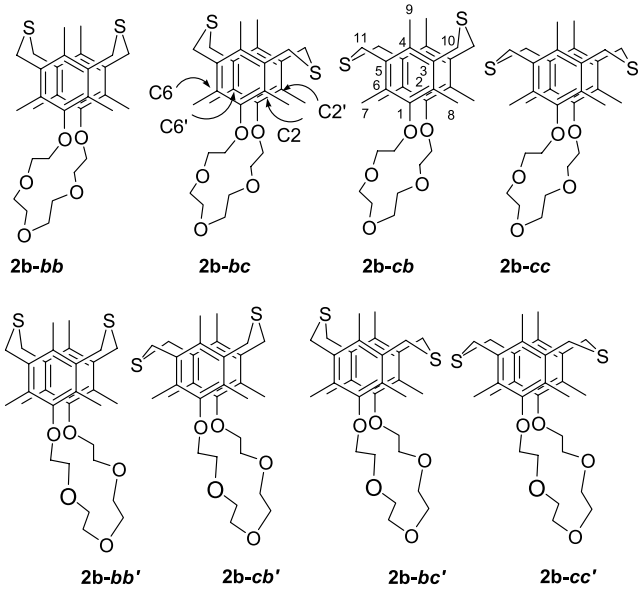

Figure 6. Possible conformations of **2b** in solution.

Table 2. The coalescence temperature and activation energy of **2a**–**b**

	T_c (K)	$\Delta\nu$ (Hz)	k_c (Hz)	$\Delta G_c^{\neq}$ (kcal mol^{-1})
2a	186	30	60	9.21
2b	186	34	76	8.80

Possible conformational processes of the three bridges in **2b** are illustrated in Figure 6. The large crown ether unit is expected to undergo the extreme 'left to right' swing resulting in the two series of conformers **2b**-*bb*–**2b**-*cc* and **2b**-*bb*′–**2b**-*cc*′ (**2b**-*bb* is equivalent to **2b**-*bb*′, **2b**-*bc* to **2b**-*cb*′, **2b**-*cb* to **2b**-*bc*′ and **2b**-*cc* to **2b**-*cc*′). The crown ether link is relatively longer and more flexible and thus would involve a much lower energy barrier. On the other hand, it could be assumed that the resolution of the proton signals of methyl groups at aromatic C2/C2′ and C6/C6′ is dependent only on the restricted conformational changes of the thia-bridges. There should be no resolution of these methyl proton signals if the frozen conformation is either **2b**-*bb* ⇔ **2b**-*bb*′ or **2b**-*cc* ⇔ **2b**-*cc*′ due to their symmetry. Thus, it could be concluded that the experimentally observed frozen conformer of **2b** in the dynamic NMR study was **2b**-*bc* ⇔ **2b**-*cb*′ and **2b**-*cb* ⇔ **2b**-*bc*′ (**2b**-*cb* ⇔ **2b**-*bc*′ is not identical to **2b**-*bc* ⇔ **2b**-*cb*′ and the two pairs are not inter-converting). In fact a crystallographic structure of **2b** also indicates the same conformational preference in the solid state. The two resolved methyl proton signals for **2b** at the low temperature limit appeared at δ 2.29 and 2.24, respectively. In **2b**-*bc* ⇔ **2b**-*cb*′ or **2b**-*cb* ⇔ **2b**-*bc*′, one of the sulfur atoms is in close proximity to the methyl groups attached to aromatic C2/C2′ and C6/C6′ for **2b**-*bc*, **2b**-*cb*′, **2b**-*cb* and **2b**-*bc*′, (the methyl groups at C6/C6′ and C2/C2′). The anisotropic effect of this sulfur atom might induce a small downfield shift of the methyl signal concerned, thus resulting in its resolution from the signal of the methyl groups at C2/C2′ and C6/C6′ for **2b**-*bc*/**2b**-*cb*′ or **2b**-*cb*/**2b**-*bc*′, respectively, in **2b**-*bc* ⇔ **2b**-*cb*′ or **2b**-*cb* ⇔ **2b**-*bc*′.

Table 3. The selected chemical shifts of **2b**[a] at 298 and at 178 K

	Chemical shift	
	298 K	178 K
C(1)	152.55	155.98, 149.95
C(3,5)	132.09	131.01, 130.45
C(4)	130.24	129.09, 128.43
C(2,6)	127.44	126.35
C(10,11)	30.83	29.75, 29.56, 29.49, 29.35
C(9)	17.80	17.26, 17.05
C(7,8)	12.31	11.97, 11.86, 11.16, 11.02

[a] The numbering of carbon atoms is shown in Figure 6.

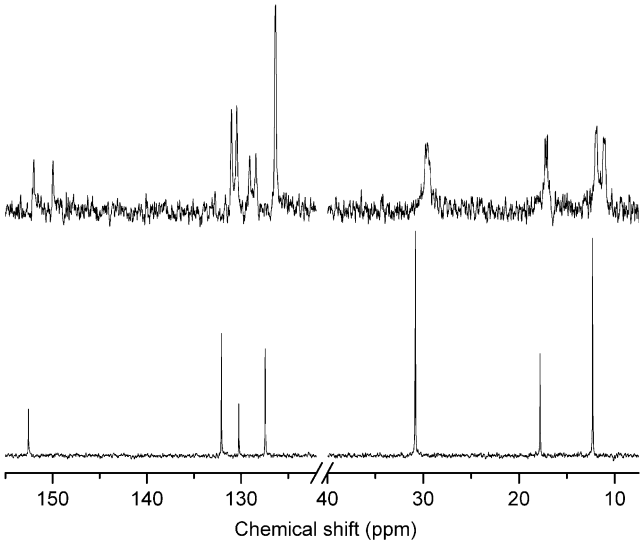

Figure 7. ^{13}C NMR spectra of **2b** (a) at 298 K and (b) at 178 K in CD_2Cl_2.

^{13}C NMR spectrum of **2b** was measured at 178 K and the assignment of selected carbon signals is listed in Table 3 It was worthy to note that while only an averaged singlet at δ 12.31 was observed at room temperature for the methyl carbons attached to C2, 2′, 6 and 6′, however, four singlets with a 1:1 ratio appeared in the spectrum taken at 178 K at δ 11.97, 11.86, 11.16 and 11.02, respectively. Simultaneously, the singlet at 30.83 corresponding to the bridge carbon emerged as four singlets. Moreover, three aromatic carbon signals were separated to two sets of singlets in a 1:1 ratio (Fig. 7). It implies that two conformers (**2b**-*bc* or **2b**-*cb*′ and **2b**-*cb* or **2b**-*bc*′) exist at this temperature. It is clear that there are two pairs of relatively well-resolved ($\Delta\delta \approx 0.8$ ppm) methyl signals. This is also consistent with the argument that the anisotropic effect of sulfur results in the deshielding of the carbons in close proximity.

2.4. Computational study of conformers

A series of DFT calculations (BLYP/DNP) were performed to determine the relative energy for the different conformers of **126-CPs** and **135-CPs** together with *syn*-9,18-dimethoxy[3.3]**MCP** (**17**) for comparison, and the results are summarized in Table 4. For both series, all *cc* conformers had the global minimum energy. The *bc*, *cb* and *bb* conformers of **126-CPs** series had a higher energy by 4.30–11.91 kcal mol^{-1} than their corresponding *cc* conformers. The electronic repulsion and steric hindrance between sulfur and phenolic oxygen accounts for the high-energy difference among conformers in **126-CPs** series. The global energy minimum conformers of **126-CPs** exactly responded to the structures in solution and in the solid state. In contrast, the differences (0.89–3.69 kcal mol^{-1}) between *cc* and other conformers in **135-CPs** series were much less than those in **126-CPs** series. The relative population of these conformers (Table 5) was thus estimated based on the data of Table 4. It was shown that the total population of *bb*, *bc* and *cb* conformers was found to be negligible for **126-CPs**. In contrast, there were more than totally 37 and 36% of *bc* and *cb* conformers, for example, for **2a** and **2b**, respectively. The calculated ratio of *cc*:(*bc*/*cb*) (63:37) for **2a** is approximately close to the experimental value (70:30) in the solid state, however, the order of conformers ratio of *cc*:(*bc*/*cb*) (63:36) for **2b** was reversed when compared to

Table 4. The relative energy (kcal mol^{-1}) of conformers of **1a–d**, **2a–c** and compound **17** (BLYP/DNP)

CP	**1a**	**1b**	**1c**	**1d**	**2a**	**2b**	**2c**	**17**
bb	11.24	11.91	9.23	8.50	2.90	2.51	3.69	10.28
bc	7.37	5.22	5.19	4.30	0.89	1.09	1.60	5.65
cb	5.69	5.10	4.93	4.36	1.60	1.24	2.02	
cc	0	0	0	0	0	0	0	0

Table 5. The population of conformers of **1a–d** and **2a–c** at 298 K[a]

CP	1a	1b	1c	1d	2a	2b	2c
bb	0	0	0	0	0	1	0
bc	0	0	0	0	28	20	11
cb	0	0	0	0	9	16	6
cc	100	100	100	100	63	63	83

[a] The population was calculated based on the data of Table 4.

the experimental values (15:85). The discrepancy in calculated and experimental population may be a consequence of the effect of crystal packing as mentioned above.

3. Conclusions

We have demonstrated that the preferential conformations of **126-CPs** were *cc* as a result of the electronic repulsion between sulfur and internal phenolic oxygen, while **135-CPs** had a tendency to take *cc* and *bc* conformations. Dynamic NMR analyses in solution were in agreement with the analyses of conformation by X-ray crystallography. The conformational barriers for the wobbling-process estimated by variable-temperature ^{1}H NMR, were 9.21 and 8.80 kcal mol^{-1}, respectively, for **2a** and **2b**, less than that of [3$_3$](1,3,5)**CP**. The ^{13}C NMR spectra at low temperature suggested two conformers with a 1:1 ratio coexisted, corresponding to the results in the solid state. The DFT calculations provided the evidence on the conformational analysis of **126-CPs** and **135-CPs**.

4. Experimental

4.1. General

The NMR spectra were determined on a Bruker ACF (300 MHz) FT-NMR spectrometer, operating at 300.13 and 75.47 MHz for ^{1}H and ^{13}C, respectively in $CDCl_3$ at room temperature. The temperature-dependent NMR experiments were performed on a Bruker AMX (500 MHz) NMR spectrometer in CD_2Cl_2. All chemical shifts are reported in ppm downfield from tetramethylsilane as an internal standard. Infrared spectra were recorded on a Perkin–Elmer 1310 infrared spectrometer. Mass spectra were determined on a VG Micromass 7035 mass spectrometer at 70 eV with electron impact or on a Finnegan TSQ mass spectrometer with electrospraying ionization (ESI). Relative intensities are given in parenthesis. Microanalysis was performed by the Microanalytical Laboratory of the Department of Chemistry, National University of Singapore.

4.2. Calculation method

The structures of **135-CPs** and **126-CPs** series were optimized using the density functional theory electronic structure program-DMol^3 available as part of Materials Studio (Accelrys Inc).[29,30] In this code electronic wave function is expanded in a localized atom-centered basis set with each basis function defined numerically on a dense radial grid. All-electron calculations were performed with a double numeric polarized (DNP) basis set (which is analogous to the Gaussian 6-31(d,p) basis set), the most complete set available in the code. The gradient-corrected BLYP functional,[31,32] a finite basis-set cutoff of 4.0 Å and a 'fine' quality (convergence tolerances: energy 1.0×10^{-5} Ha; maximum force 0.002 Ha/Å; maximum displacement 0.005 Å. SCF tolerance: 1.0×10^{-6}) were used. During modeling, the crown moiety in cyclophane was maintained to tilt to one side and two thia-bridges took *cc*, *bc* or *bb* conformation during the calculation.

4.2.1. 1,8-Bis(2,6-diformylphenoxyl)-3,6-dioxaoctane (5a). A mixture of 2,6-diformylphenol (300 mg, 2.0 mmol), triethylene glycol dibromide (276 mg, 1.0 mmol) and anhydrous K_2CO_3 (500 mg) was stirred in dry DMF (10 mL) at 60–70 °C under nitrogen for 24 h. The reaction mixture was poured into ice water (50 mL) and stirred for 30 min. The resulting precipitate was collected by filtration and washed with water. The crude product was purified by chromatography on silica gel using ethyl acetate and hexane (2:3) as eluent to give **5a** (210 mg, 51%) as a light yellow solid: mp 120–121.5 °C; ^{1}H NMR 3.64 (oxyethylene, s, 4H), 3.83 (oxyethylene, m, 4H), 4.33 (oxyethylene, m, 4H), 7.34 (aromatic, t, 2H, $J=7.6$ Hz), 8.59 (aromatic, d, 4H, $J=7.6$ Hz), 10.44 (–C*H*O, s, 4H); IR (KBr) 1676 cm^{-1} (–CHO); MS (ESI) (*m*/*z*) 437.2 (M+ Na$^+$, 93); Anal. Calcd for $C_{22}H_{22}O_8$: C, 63.76; H, 5.35. Found: C, 63.89; H, 5.55.

4.2.2. 1,8-Bis(2,6-dihydroxyphenoxyl)-3,6-dioxaoctane (5b). A mixture of compound **5a** (150 mg, 3.62 mmol) and sodium borohydride (100 mg) in THF (10 mL) was heated at reflux for 1 h. The mixture was cooled and the THF was removed under reduced pressure. The residue was extracted with $CHCl_3$ and the organic layer was washed, dried and evaporated to afford tetrol **5b** (145 mg, 95%) as a colorless oil: ^{1}H NMR δ 3.42 (–O*H*, br. s, 4H), 3.69 (oxyethylene, s, 4H), 3.73–3.76 (oxyethylene, m, 4H), 4.03–4.06 (oxyethylene, m, 4H), 4.58 (–CH_2OH, s, 8H), 6.98 (aromatic, t, 2H, $J=7.6$ Hz), 7.18 (aromatic, d, 4H, $J=$ 7.6 Hz); MS (EI) (*m*/*z*) 368.1 (M$^+-3H_2O$, 12); IR (KBr) 3364 cm^{-1} (–OH); Anal. Calcd for $C_{22}H_{30}O_8$: C, 62.55; H, 7.16. Found: C, 62.30; H, 7.30.

4.2.3. 1,8-Bis(2,6-dibromomethylphenoxyl)-3,6-dioxaoctane (5c). PBr_3 (1.0 g, 3.7 mmol) was added to a solution of **5b** (0.20 g, 0.47 mmol) in dry 1,4-dioxane (10 mL) at 0 °C. The mixture was further stirred for 5 h at 0 °C, and then the mixture was poured into ice water/dichloromethane. The organic layer was separated and the water layer was extracted three times with dichloromethane. All organic layers were combined and washed with 10% $NaHCO_3$, water, and then evaporated. The residue was chromatographed on silica gel using ethyl acetate/hexane (9:1) as eluent to yield the product **5c** (0.24 g, 75%) as a white solid: mp 115–116 °C (lit.: 116–117 °C[33]); ^{1}H NMR δ

3.87 (oxyethylene, s, 4H), 3.95–3.98 (oxyethylene, m, 4H), 4.30–4.33 (oxyethylene, m, 4H), 4.64 (–CH_2Br, s, 8H), 7.11 (aromatic, t, 2H, J=7.6 Hz), 7.41 (aromatic, H, d, 4H, J=7.6 Hz).

4.2.4. 18,27-Dithia-1,4,7,10-tetraoxa-[10.3.3](1,2,6)cyclophane (1a). A solution of 95% sodium sulfide nonahydrate (480 mg, 2.0 mmol) in 95% ethanol (300 mL) and a solution of **5c** (674 mg, 1.0 mmol) in benzene (300 mL) in separate rotaflow dropping funnels were added dropwise simultaneously at the same rate to nitrogen purged 95% ethanol (1 L). After the addition, the mixture was stirred for another 15 h and the bulk of the solvent was removed under reduced pressure. Water and dichloromethane were added to the residue, and the mixture was stirred until all solids dissolved. The organic layer was separated, dried, and evaporated. The residue was chromatographed on silica gel using ethyl acetate/dichloromethane (1:40) as eluent to yield **1a** (140 mg, 33%) as colorless crystals: mp 213–215 °C; ^{1}H NMR ($CDCl_3$) δ 3.34 (–CH_2SCH_2–, d, 4H, J=14.5 Hz), 3.66–3.69 (oxyethylene, m, 4H), 3.92–3.95 (oxyethylene, m, 8H), 4.55 (–CH_2SCH_2–, d, 4H, J=14.5 Hz), 6.64 (aromatic, t, 2H, J=7.6 Hz), 6.97 (aromatic, d, 4H, J=7.6 Hz); ^{13}C NMR δ 155.28, 131.09, 129.19, 123.99, 73.15, 69.85, 69.24, 30.35; MS (EI) (*m*/*z*) 418 (M^+, 77); Anal. Calcd for $C_{22}H_{26}O_4S_2$: C, 63.13; H, 6.26; Found: C, 63.30; H, 6.30.

4.2.5. 1,8-Bis(4-methyl-2,6-dihydroxymethylphenoxyl)-3,6-dioxaoctane (7a). Triethylene glycol dibromide (4.92 g, 17.8 mmol) was added under nitrogen to a suspension of anhydrous K_2CO_3 (10 g, 72.4 mmol) and 2,6-dihydroxymethylphenol (6.0 g, 35.7 mmol) in acetone (70 mL). The mixture was maintained at gentle reflux for 5 days and the acetone was then removed under reduced pressure. The residue was poured into a mixture of water and dichloromethane. The organic layer was washed, dried, and then evaporated. The residue was chromatographed on silica gel using ethyl acetate/dichloromethane (15:85, then 40:60) as eluent to yield **7a** (5.35 g, 67%) as a colorless oil which crystallized on long standing when kept at 0 °C: mp 93–96 °C; ^{1}H NMR δ 2.28 (methyl, s, 6H), 3.78 (oxyethylene, s, 4H), 3.82–3.86 (oxyethylene, m, 4H), 4.12–4.15 (oxyethylene, m, 4H), 4.64 (–CH_2OH, s, 8H), 7.07 (aromatic, s, 4H); IR (KBr) 3387 cm^{-1} (–OH); MS (EI) (*m*/*z*) 414 (M^+-2H_2O, 7), 396 (M^+-3H_2O, 48). Anal. Calcd for $C_{24}H_{34}O_8$: C, 63.98; H, 7.61, 28.41. Found: C, 63.75; H, 7.77.

4.2.6. 1,8-Bis(4-methyl-2,6-dibromomethylphenoxyl)-3,6-dioxaoctane (7b). The preparation of **7b** follows the similar synthetic procedure of **5b**: mp 97–98 °C; ^{1}H NMR δ 2.29 (methyl, s, 6H), 3.86 (oxyethylene, s, 4H), 3.93–3.96 (oxyethylene, m, 4H), 4.26–4.28 (oxyethylene, m, 4H), 4.60 (–CH_2Br, s, 8H), 7.16 (aromatic, s, 4H); MS (EI) (*m*/*z*) 698 (M^+, 1), 700 (M^++2, 4), 702 (M^++4, 5.4), 704 (M^++6, 4), 706 (M^++8, 1); Anal. Calcd for $C_{24}H_{30}Br_4O_4$: C, 41.06; H, 4.31. Found: C, 40.90; H, 4.50.

4.2.7. 18,27-Dithia-14,22-dimethyl-1,4,7,10-tetraoxa-[10.3.3](1.2.6)cyclophane (1b). The preparation of **1b** follows the similar synthetic procedure of **1a**. Tetrabromide **7b** (700 mg, 1.0 mmol) reacted with sodium sulfide nonahydrate (480 mg, 2.0 mmol) to yield **1b** (140 mg, 31%) as colorless crystals: mp 223–225 °C; ^{1}H NMR δ 2.11 (methyl, s, 6H), 3.29 (–CH_2SCH_2–, d, 4H, J=14.5 Hz), 3.63–3.66 (oxyethylene, m, 4H), 3.90–3.92 (oxyethylene, m, 4H), 3.96 (oxyethylene, s, 4H), 4.51 (–CH_2SCH_2–, d, 4H, J=14.5 Hz), 6.80 (aromatic, s, 4H); ^{13}C NMR δ 153.34, 133.01, 130.52, 129.74, 73.26, 69.95, 69.39, 30.29, 20.57; MS (EI) (*m*/*z*) 446 (M^+, 23); Anal Calcd for $C_{24}H_{30}O_4S_2$: C, 64.54; H, 6.77. Found: C, 64.70; H, 6.50.

4.2.8. 2,4,6-Trimethyl-3,5-bis(bromomethyl)anisole (9). 2,4,6-Trimethylanisole (10 g, 66.6 mmol) was added to a mixture of 47% aq HBr (40 mL) and glacial acetic acid (180 mL), followed by 1,3,5-trioxane (18.0 g, 0.20 mol) and tetradecyltrimethyl ammonium bromide (0.50 g). The mixture was heated up and the temperature kept at 95 °C for 5 h (thin layer chromatography (TLC) was performed to monitor the completeness of the reaction). After cooling to room temperature, the white precipitate was filtered, washed with plenty of water and then dissolved in dichloromethane. The organic layer was washed with 5% bicarbonate, water and dried. The organic solvent was removed under the reduced pressure and residue was chromatographed on silica gel using ethyl acetate and hexane (10:90) as eluent to afford the pure **9** (8.3 g, 31%) as a white solid: mp 137–138.5 °C; ^{1}H NMR δ 2.36 (methyl, s, 6H), 2.42 (methyl, s, 3H), 3.67 (methoxy, s, 3H), 4.57 (–CH_2Br, s, 4H); MS (EI) (*m*/*z*) 338 (M^++4, 70), 336 (M^++2, 83), 334 (M^+, 72), 176 (M^+-2^{79}Br); Anal. Calcd for $C_{12}H_{16}Br_2O$: C, 42.89; H, 4.80. Found: C, 43.10; H, 4.65.

4.2.9. 2,4,6-Trimethyl-3,5-bis(mercaptomethyl)anisole (10). Compound **9** (3.63 g, 10.9 mmol) was added to a stirred solution of thiourea (1.65 g, 23.6 mmol) in absolute ethanol (40 mL). After addition, the mixture was continued to reflux for another 2 h, and then the mixture was cooled to room temperature, filtered and dried under vacuum to give 2,4,6-trimethyl-3,5-bis(isothioureamethyl)anisole dibromide crude salt (5.0 g). The salt was used in the next step without further purification. A solution of 5.0 g of salt in 20% KOH (50 mL) was boiled under reflux for 5 h. After the mixture was cooled to room temperature, 9 M aqueous H_2SO_4 was added to neutralize the alkaline solution until pH to 7. The neutralized mixture was extracted with dichloromethane. The organic layer was washed with water, dried and concentrated. The residue was chromatographed on silica gel using ethyl acetate and hexane as eluent (1:9) to give **10** (2.17 g, 83%) as a pale yellowish solid: mp 109–110 °C; ^{1}H NMR δ 1.59 (–SH, t, 2H, J=6.4 Hz), 2.34 (methyl, s, 6H), 2.40 (methyl, s, 3H) 3.66 (methoxy, s, 3H), 3.77 (–CH_2SH, d, 4H, J=6.4 Hz); MS (EI) (*m*/*z*) 242 (M^+, 87); Anal. Calcd for $C_{12}H_{18}OS_2$: C, 59.46; H, 7.48. Found: C, 59.70; H, 7.30.

4.2.10. 2,11-Dithia-5,7,9,14,16,18-hexamethyl-6,15-dimethoxy[3.3](1,3)cyclophane (11/13). A solution of dibromide **9** (3.00 g, 8.93 mmol) and dithiol **10** (2.16 g, 8.93 mmol) dissolving in benzene (500 mL) were slowly added dropwise to 95% ethanol (1500 mL) over 8 h. The resulting solution was stirred for another 16 h, and then the bulky solvent was removed under the reduced pressure. Dichloromethane was added to the residue and stirred. The organic solvent was washed with dilute hydrochloric acid

and water. The dichloromethane was removed and the residue was chromatographed on silica gel using dichloromethane and hexane (1:1) to give *anti*-isomer (1.83 g, 49%) and *syn*-isomer (0.363 g, 10%) as colorless crystals and white solid, respectively.

4.2.11. *anti*-2,11-Dithia-5,7,9,14,16,18-hexamethyl-6,15-dimethoxy[3.3](1,3)cyclophane (11). Mp >240 °C (decomposed); ^{1}H NMR δ 1.21 (methyl, s, 6H), 2.44 (methyl, s, 12H), 3.69 (methoxy, s, 6H), 3.67 (–C*H*$_2$SC*H*$_2$–, d, 4H, J=13.7 Hz), 3.78 (–C*H*$_2$SC*H*$_2$–, d, 4H, J=13.7 Hz); MS (ESI) no molecular ion peak was observed MS (EI) (*m*/*z*) 416 (M^+, 75); Anal. Calcd for $C_{24}H_{32}O_2S_2$: C, 69.19; H, 7.74. Found: C, 69.33; H, 7.64.

4.2.12. *syn*-2,11-Dithia-5,7,9,14,16,18-hexamethyl-6,15-dimethoxy[3.3](1,3)cyclophane (13). Mp >240 °C (decomposed); ^{1}H NMR δ 2.07 (methyl, s, 6H), 2.34 (methyl, s, 12H), 3.61 (methoxy, s, 6H), 3.70 (–C*H*$_2$SC*H*$_2$–, s, 8H); MS (EI) (*m*/*z*) no molecular ion peak was observed; Anal. Calcd for $C_{24}H_{32}O_2S_2$: C, 69.19; H, 7.74. Found: C, 69.50; H, 7.90.

4.2.13. *anti*-2,11-Dithia-5,7,9,14,16,18-hexamethyl-6,15-dihydroxy[3.3](1,3)cyclophane (12). 1 M BBr_3/CH_2Cl_2 (2.0 mL, 2.0 mmol) was added to the solution of anti-**11** (100 mg, 0.24 mmol) in $CHCl_3$ (5 mL) at −78 °C. The mixture was stirred at −78 °C for 3 h, and then stirred overnight at room temperature. The water was added to the mixture, and then extracted with CH_2Cl_2. The organic layer was washed with water, dried and filtered. CH_2Cl_2 was removed and the residue was chromatographed on silica gel using dichloromethane and acetone (3:1) as eluent to give **12** (10 mg, 11%) as a white solid: mp 250 °C (decomposed); ^{1}H NMR δ 1.21 (methyl, s, 6H), 2.38 (methyl, s, 12H), 3.67 (–CH_2SCH_2–, d, 4H, J=13.8 Hz), 3.78 (–CH_2SCH_2–, d, 4H, J=13.8 Hz) 4.55 (–OH, s, 2H); IR (KBr) 3545 cm^{-1} (–OH); MS (EI) (*m*/*z*) 388 (M^+, 66); Anal. Calcd $C_{22}H_{28}O_2S_2$ for: C, 68.00; H, 7.26. Found: C, 67.90; H, 7.41.

5. Supporting materials

Crystallographic data for the structures reported in this paper have been deposited with the Cambridge Crystallographic Data Center as supplementary publication numbers CCDC-245673 (**1a**) and 245672 (**1b**). Copies of the data can be obtained free of charge upon application to CCDC, 12 Union Road, Cambridge CB2 1EZ, UK (fax: +44 1223 33603; e-mail: deposit@ccdc.cam.ac.uk).

Acknowledgements

We are grateful to the National University of Singapore (NUS) for financial support. Assoc. Prof. J. J. Vittal and Ms. Tan Geok Kheng are acknowledged for determining the X-ray crystallographic structures in the X-ray Diffraction Laboratory at the Department of Chemistry, NUS.

References and notes

1. Mitchell, R. H. In *Cyclophanes*; Keehu, P. M., Rosenfeld, S. M., Eds.; Organic Chemistry; Academic: New York, 1983; Vol. 45-I, Chapter 4.
2. Mitchell, R. H. *J. Am. Chem. Soc.* **2002**, *124*, 2352–2357.
3. Mitchell, R. H.; Vinod, T. K.; Bodwell, G. J.; Weerawarna, K. S.; Anker, W.; Williams, R. V.; Bushnell, G. W. *Pure Appl. Chem.* **1986**, *58*, 15–24.
4. Fukazawa, Y.; Takeda, Y.; Usui, S.; Kodama, M. *J. Am. Chem. Soc.* **1988**, *110*, 7842–7847.
5. Semmelhack, M. F.; Harrison, J. J.; Young, D. C.; Gutiérrez, A.; Rafii, S.; Clardy, J. *J. Am. Chem. Soc.* **1985**, *107*, 7508–7514.
6. Sako, K.; Shinmyozu, T.; Takemura, H.; Suenaga, M.; Inazu, T. *J. Org. Chem.* **1992**, *57*, 6536–6541.
7. Takemura, H.; Kariyazono, H.; Kon, N.; Shinmyozu, T.; Inazu, T. *J. Org. Chem.* **1999**, *64*, 9077–9079.
8. Moriguchi, T.; Sakata, K.; Tsuge, A. *J. Chem. Soc., Perkin Trans. 2* **2001**, 934–938.
9. Sako, K.; Tatemitsu, H.; Onaka, S.; Takemura, H.; Osada, S.; Wen, G.; Rudzinski, J. M.; Shinmyou, T. *Liebigs Ann.* **1996**, 1645–1649.
10. Newkome, G. R.; Pappalardo, D.; Fronczek, F. R. *J. Am. Chem. Soc.* **1983**, *105*, 5152–5153.
11. Bodwell, G. J.; Bridson, J. N.; Houghton, T. J.; Yarlagadda, B. *Tetrahedron Lett.* **1997**, *38*, 7475–7478.
12. Boekelheide, V.; Hollins, R. A. *J. Am. Soc. Chem.* **1973**, *95*, 3201–3208.
13. Hanson, A. W.; Macaulay, E. W. *Acta Crystallogr.* **1972**, *B28*, 1255–1260.
14. Meno, T.; Sako, K.; Suenaga, M.; Mouri, M.; Shinmyozu, T.; Inazu, T.; Takemura, H. *Can. J. Chem.* **1990**, *68*, 440–445.
15. Koga, T.; Yasutake, M.; Shinmyozu, T. *Org. Lett.* **2001**, *3*, 1419–1422.
16. Bodwell, G. J.; Bridson, J. N.; Houghton, T. J.; Kennedy, J. W. J.; Mannion, M. R. *Angew. Chem., Int. Ed.* **1996**, *35*, 1320–1321.
17. Bodwell, G. J.; Houghton, T. J.; Kennedy, J. W. J.; Mannion, M. R. *Angew. Chem., Int. Ed.* **1996**, *35*, 2121–2123.
18. Xu, J.; Lai, Y.-H. *Org. Lett.* **2002**, *4*, 3211–3214.
19. Xu, J.; Lai, Y.-H. *Tetrahedron Lett.* **2002**, *43*, 9199–9202.
20. Xu, J.; Lai, Y.-H.; Wang, W. *Org. Lett.* **2003**, *5*, 2781–2784.
21. Zondervan, C.; van den Beuken, E. K.; Kooijman, H.; Spek, A. L.; Feringa, B. L. *Tetrahedron Lett.* **1997**, *38*, 3111–3114.
22. Mitchell, R. H.; Iyer, V. S. *Synlett* **1989**, 55–57.
23. Anker, W.; Beveridge, K. A.; Bushnell, G. W.; Mitchell, R. H. *Can. J. Chem.* **1984**, *62*, 661–666.
24. Anker, W.; Bushnell, G. W.; Mitchell, R. H. *Can. J. Chem.* **1979**, *57*, 3080–3087.
25. Karle, I. L.; Estlin, J. A.; Britts, K. *Acta Crystallogr.* **1967**, *22*, 273–280.
26. Davis, B. R.; Bernal, I. *J. Chem. Soc. B* **1971**, 2307–2313.
27. Calder, I. C.; Garratt, P. J. *J. Chem. Soc. B* **1967**, 660–662.
28. Vögtle, F.; Neumann, P. *J. Chem. Soc., Chem. Commun.* **1970**, 1464–1465.
29. Delley, B. *J. Chem. Phys.* **1990**, *92*, 508–517.
30. Delley, B. *J. Chem. Phys.* **2000**, *113*, 7756–7764.
31. Lee, C.; Yang, W.; Parr, R. G. *Phys. Rev. B* **1988**, *37*, 785–789.
32. Becke, A. D. *J. Chem. Phys.* **1988**, *88*, 2547–2553.
33. Alston, D. R.; Slawin, A. M. Z.; Stoddart, J. F.; Williams, D. J. *Angew. Chem., Int. Ed. Engl.* **1984**, *23*, 821–823.